

## Article

# Reducing the Environmental and Economic Consequences of Installing an Underground Collector and Increasing User Comfort with a New Geometry and Installation Method

Lubomíra Gabániová \* and Dušan Kudelas 

Institute of Earth Resources, Faculty of Mining, Ecology, Processing Control and Geotechnology, Technical University of Kosice, Letna 1/9, 040 01 Kosice, Slovakia; dusan.kudelas@tuke.sk

\* Correspondence: lubomira.gabaniova@tuke.sk

**Abstract:** The installation of ground collectors often has several disadvantages for the user, despite future benefits in more ecological heating, namely the need for a large space for installation, which increases costs, and can also cause inconvenience later, for example, by keeping snow on the surface for a longer time. The goal of this paper was to find out with the help of simulations in ANSYS whether a collector with a different geometry and arrangement (vertical spiral with diameters of 6, 8 and 10 m), which would be more comfortable, cheaper, and also friendlier to the environment, would achieve performance similar to the classic geometry—meander. The initial results are relatively favorable and prove that there is room for optimization and improvement in this field. Verification of network sensitivity in all cases is 8% or less. In the current situation of the energy crisis, it is necessary to look for the possibilities of using heat pumps in cities and metropolises. The new geometry could increase the attractiveness and availability of ground source heat pumps in general, which would support efforts to reduce emissions and possibly also reduce the negative impacts of heating on the environment.

**Keywords:** ground collector; heat extraction; CFD; renewable energy sources



**Citation:** Gabániová, L.; Kudelas, D. Reducing the Environmental and Economic Consequences of Installing an Underground Collector and Increasing User Comfort with a New Geometry and Installation Method. *Processes* **2023**, *11*, 2723. <https://doi.org/10.3390/pr11092723>

Academic Editor: Iztok Golobič

Received: 15 August 2023

Revised: 5 September 2023

Accepted: 9 September 2023

Published: 12 September 2023



**Copyright:** © 2023 by the authors. Licensee MDPI, Basel, Switzerland. This article is an open access article distributed under the terms and conditions of the Creative Commons Attribution (CC BY) license (<https://creativecommons.org/licenses/by/4.0/>).

## 1. Introduction

Horizontal ground source heat pumps are an excellent choice for environmentally friendly heating of buildings due to their high efficiency, and attention should therefore be paid to making this technology available to as many users as possible in all types of locations, especially in cities and metropolises. In general, heat pumps are among the essential mitigation and adaptation measures in reducing emissions and achieving zero-carbon human society and their share of heating is expected to be more than 50% by 2060, although in 2014 it was only 3.4% [1,2]. It is therefore meaningful to observe the geometry and installation options of ground source collectors, which, compared to air-source heat pumps, occupy a large area of land and require a lot of earthworks and site modifications. This research investigates the possibilities of reducing the burial area of ground collectors while achieving performances similar to classical geometries, using ANSYS FLUENT R19.2.

There are many studies on ground collectors and their modeling and simulation using computational fluid dynamics. It is an efficient, fast, accessible, and reasonably costly tool for wide use with sufficient flexibility. It is crucial knowledge that the experimental results of many studies are in very good agreement with the CFD results, with deviations fluctuating between 2 and 10%. This is the reason why CFD simulation results without experiment should not be undervalued or totally rejected [3].

The power of the effect of soil temperature and the surrounding climate on year on performance of meander ground heat exchangers is underlined in Hepburn et al. [4].

Benazza et al. also studied the importance of ground collector geometry and thermal conductivities on their efficiency and performance with ANSYS Fluent [5]. Results of the

research provided by Garcia et al. referred to soil–collector interaction, and the effect of collectors' operation on ground temperature and humidity. They found that heat extraction by the collector has a substantial effect on the ground in close proximity to the pipe [6].

Similar to the authors of this paper, Sanaye et al. tried to optimize the design of horizontal ground collectors by using ANSYS with the finite element method, for example by improving the installation area and looking at the pipe row's interaction [7].

Another study with numerical simulation in ANSYS was made by Chong et al. They created 10 cases with a 3D numerical model horizontal ground collector and examined the effect of spacing between loops, their diameters, and three types of soil. The conclusion of that study was that type of soil is critical for collector performance; spacing between loops can influence its thermal performance significantly and the diameter of loops have some effect, too, but not that much [8].

Fluent was used to analyze three geometries of ground collector (linear, slinky, and 3D spiral) in different operating conditions by Condego et al. They also confirm that the type of soil and its thermal behavior is really important for the ground collector, its output, and its installation. The best performance was found with the 3D spiral collector and the worst with linear geometry [9,10].

Capozza, Zarrella, and De Carli studied the effect of the soil surface on the output of the horizontal ground collector. They found that the flow of groundwater could increase the performance of ground collectors and prolong their operational capability [11].

Research on linear and slinky ground collectors and the impact of the loop diameter and spacing on collectors' performance in ANSYS Fluent was run by Wu et al. for the United Kingdom's climate. The diameter of loops showed up again as a less crucial parameter, while geometry and spacing between loops caused a bigger difference in the operation of the collector. For example, they found that expanding the distance between loops led to higher specific heat extraction. Wu confirmed their results by experiment also in [12–14].

Like Wu, Kim, Yoon, Go, and Lee also examined horizontal ground collectors through an experiment and by numerical simulations. They concluded a very similar study, so the geometry of the collector and soil type are fundamental factors that affect their output and operation [14–16].

The most current paper on the computational investigation of earth–air heat exchangers was provided by Cirillo et al. [17] and that about horizontal spiral coil by Liu et al. [18].

All previous studies focus on classic geometries such as meanders, slinkies, and spirals, while this study presents the simulation of a new geometry, the vertical spiral.

The aim of this article is to find out whether the new design of the geometry of the ground collectors from the authors of this article could match the performance geometry of the meander, which is one of the best-known geometries of horizontal ground collectors. This goal should be achieved by numerical simulations in ANSYS Fluent, in condition of the heating season in Slovakia. The results of meander geometry are in agreement with other works with a similar focus, and comparing them with results of a new geometry, vertical spiral collector, on which there is no knowledge, is the main contribution of this paper. The need for the innovation of ground collectors' geometry and installation follows from the trend of the implementation of renewable energy sources for housing in cities, where there is not enough space to install ground collectors of meander geometry. The new design should require less space for the installation and less groundwork. The focus of this research is on numerical simulations solving this problem in the present, so there is no experiment validation with new designs yet; thus, there is space for future research in this study.

## 2. Methods of Research

Models of collectors were created in Design Modeler in ANSYS R19.2 and simulations were run in Fluent 19.2. The thermophysical properties of soil and its average temperatures at depths of 10 and 100 cm were obtained from the Slovak Hydro-meteorological Institute. The classical geometry—meander—was compared with new designs by authors of this

paper, the vertical spiral, with 3 different diameters and 2 options of spacing between pipes. The workflow in Table 1 describes the methodology of the research; in total, 75 simulations with 5 cases during 3 periods were run.

**Table 1.** Research workflow.

<b>Aim:</b>					
<b>Modeling of Ground Collectors with Meander Geometry Compared with Geometry of New Designs</b>					
Step 1	Create model in Design Modeler ANSYS R19.2				
Step 2	Meshing model in ANSYS R19.2				
Step 3	Set up FLUENT 19.2 general settings				
Period	September–November		December–February		March–May
Soil	Dry soil—sand	Moist soil—sand	Saturated soil—sand	Dry soil—clay	Wet soil—clay
Classical geometry			Meander		
New geometry	Spiral 6 m/3.75		Spiral 6 m/2.75	Spiral 8 m	Spiral 10 m

The parameters of all the cases are available in Table 2. The coil designation in the geometry name shows how many loops of pipe the given vertical spiral has. The parameters of length, width, and height are given for the whole model, i.e., for the ground in which the collector is located.

**Table 2.** Parameters of cases 1–5.

Case	Model of Collector + Ground (Length × Width × Height)	Geometry	Length of Pipe	Area of Collector	Installation Depth	Inner Pipe Diameter
1	20 m × 15 m × 3 m	Meander	142.5 m	17.91 m <sup>2</sup>	1.5 m	
2	13 m × 10 m × 4.8 m	Spiral Ø 6 m, 3.75 coils	102 m	12.82 m <sup>2</sup>	1–4 m	
3	13 m × 10 m × 4.8 m	Spiral Ø 6 m, 2.75 coils	67.4 m	8.47 m <sup>2</sup>	1–4.5 m	0.04 m
4	20 m × 15 m × 3.8 m	Spiral Ø 8 m, 3.75 coils	115.24 m	14.48 m <sup>2</sup>	1–3 m	
5	20 m × 15 m × 3.8 m	Spiral Ø 10 m, 3.75 coils	133.8 m	16.81 m <sup>2</sup>	1–3 m	

All models were meshed in Meshing ANSYS R19.2. Mesh sensitivity was analyzed in cases 1–5 (collector’s mesh cells size 0.01885 m/ground mesh cell’s size 0.3 m), which was used for rest of study and is shown in Figure 1. The number of elements is shown in Table 3. Five different meshes were created for a meander-shaped collector model in dry sand/gravel in autumn. It can be seen from Figure 1 that for the different grids, the results of the division of outlet and inlet temperatures were almost identical, with a variation of 0.62–8.02% in case 1, 0–8.11% in case 2, 2.19–4.94% in case 3, 1.2–8% in case 4, and 1.42–5% in case 5.

**Table 3.** Settings of models and simulations in FLUENT R19.2.

Wall pipe	Coupled, HDPE			
Symmetry ground	Via system coupling			
Wall ground top and bottom	Temperature			
Scheme	SIMPLE			
Model	Viscous—laminar			
Spatial discretization	Second order upwind			
Governing equations	continuity equation, heat transfer equation, Navier–Stokes equations			
Type of elements	4 node linear tetrahedron			
Case	Volume of model (collector/ground)		Number of elements (collector/ground)	
1	900 m <sup>3</sup>	(0.18 m <sup>3</sup> /899.82 m <sup>3</sup> )	5,346,156	(210,822/5,135,334)
2	624 m <sup>3</sup>	(0.11 m <sup>3</sup> /623.89 m <sup>3</sup> )	3,393,966	(21,913/3,372,053)
3	624 m <sup>3</sup>	(0.087 m <sup>3</sup> /623.91 m <sup>3</sup> )	2,765,238	(45,509/2,719,729)
4	1140 m <sup>3</sup>	(0.145 m <sup>3</sup> /1139.9 m <sup>3</sup> )	8,136,882	(194,189/7,942,693)
5	1140 m <sup>3</sup>	(0.173 m <sup>3</sup> /1139.8 m <sup>3</sup> )	5,746,903	(99,569/5,647,334)

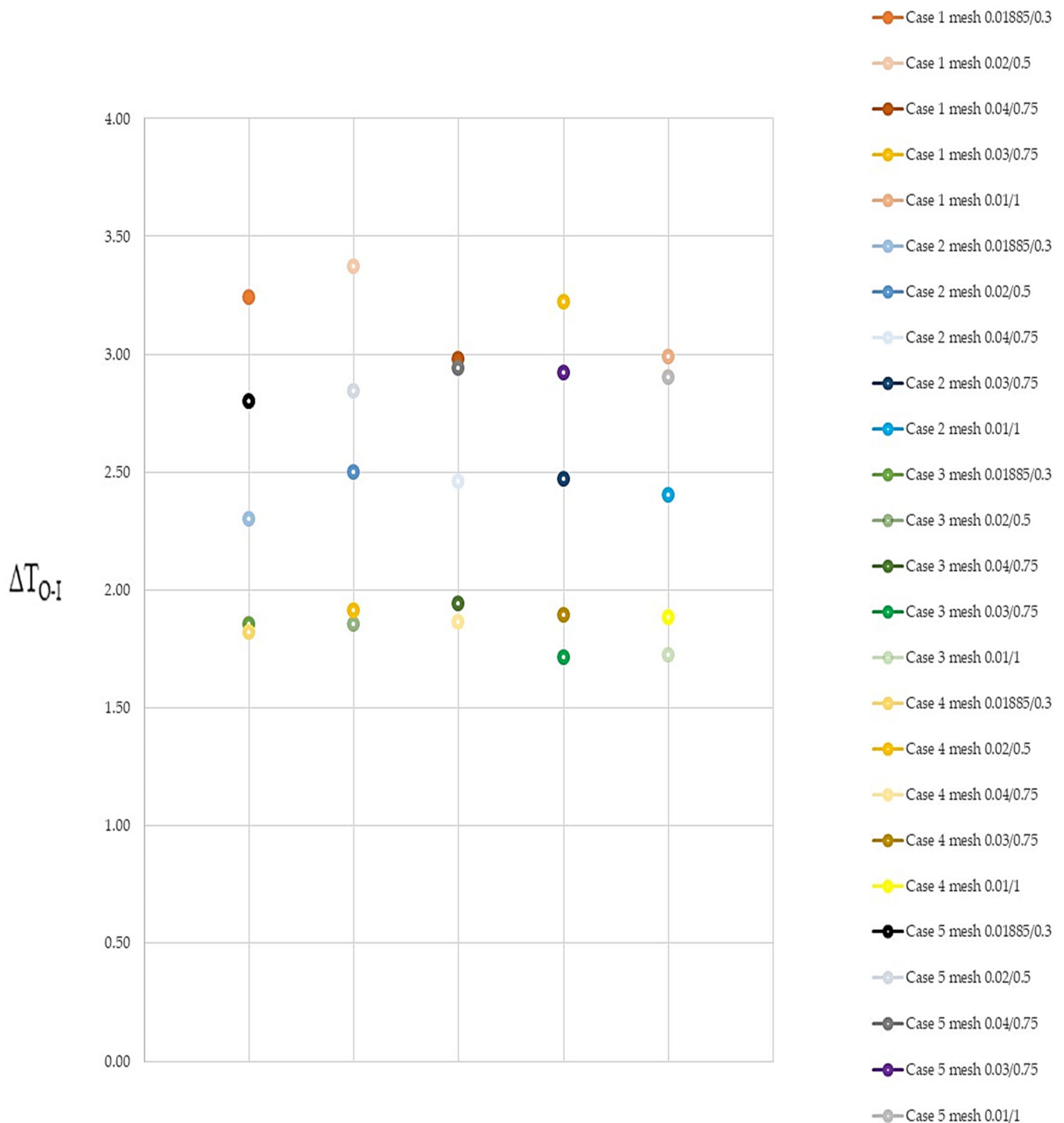


**Figure 1.** Difference in model input and output temperatures for different mesh settings; O—outlet, I—Inlet.

The first number represents the size of one collector mesh cell (m); the second number is the size of one mesh cell made for the ground in which the collector is stored (m). These sizes were set in meshing. The soft setting (Table 4) means that ANSYS could adjust the size of the cells as needed, it does not have to adhere to them strictly.

**Table 4.** Mesh conditions of cases 1–5.

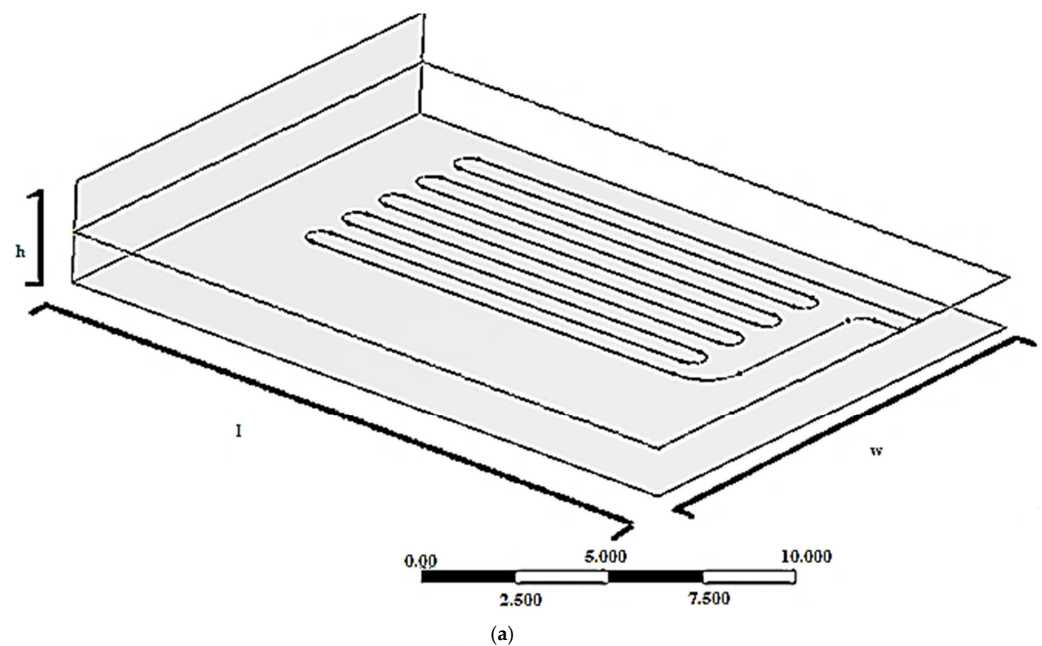
Case	Orthogonal Quality	Element Size/Behavior	
		Ground	Collector
1	4 nodes tetrahedral	Body sizing: 0.3 m/Soft	Face sizing: 0.01885 m/Soft
2	4 nodes tetrahedral	Body sizing: 0.75 m/Soft	Face sizing: 0.0189 m/Soft
3	4 nodes tetrahedral	Body sizing: 0.75 m/Soft	Face sizing: 0.0189 m/Soft
4	4 nodes tetrahedral	Body sizing: 0.3 m/Soft	Body sizing: 0.012 m/Soft
5	4 nodes tetrahedral	Body sizing: 0.3 m/Soft	Body sizing: 0.0178 m/Soft

The settings of the models and simulations in FLUENT 19.2 are available in Tables 3–5.

**Table 5.** Boundary conditions of cases 1–5.

Boundary Conditions		Material
Inlet	$0.1 \text{ m}\cdot\text{s}^{-1}$ , 269 K	-
Symmetry ground	Via system coupling	type of soil
Bottom side	2–5 m of depth Temperature September–November: 286.85 K December–February: 277.55 K March–May: 281.05 K	type of soil
	Temperature September–November: 284.95 K December–February: 273.45 K March–May: 284.65 K	type of soil

The model of meander geometry and the model of the new design, the vertical spiral, are displayed in Figure 2. The model of the meander geometry collector is placed 1.5 m below the surface, and the spacing between each row of pipe is 0.8 m.

**Figure 2.** Cont.

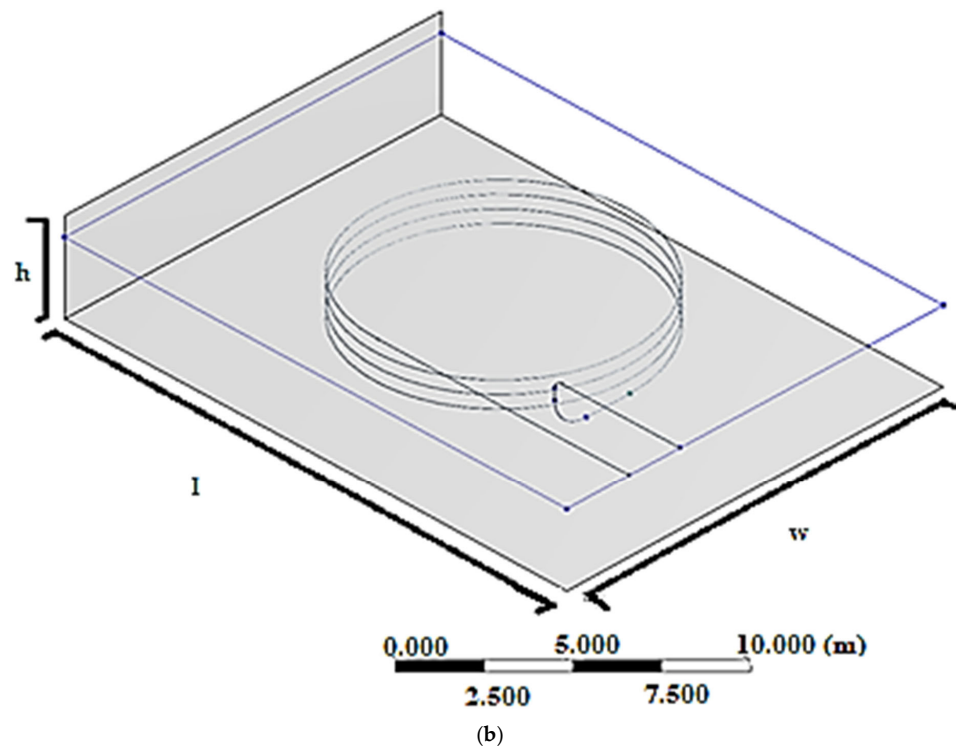


**Figure 2.** Models of meander geometry (a) and vertical spiral geometry (b).

Due to the great diversity of geological formations, height differences, and a large amount of surface water and groundwater, soil temperatures are significantly dependent on the specific place of measurement, the season, and, of course, the depth of measurement. For a better idea of the development of soil temperatures in our territory, we chose five places where the SHMU stations (Slovak Hydro-meteorological Institute) measure temperatures at a depth of 10 and 100 cm.

From the data provided by SHMU, we created a graph of temperature fluctuations in the indicated depths at the measuring points during 2017 (Figures 3 and 4). However, these data were not complete (a gap between June and July). From these data, we also calculated the average temperature for each season at depths of 10 and 100 cm, which we then used to set the input data before running the simulations (Table 6) [19–22].

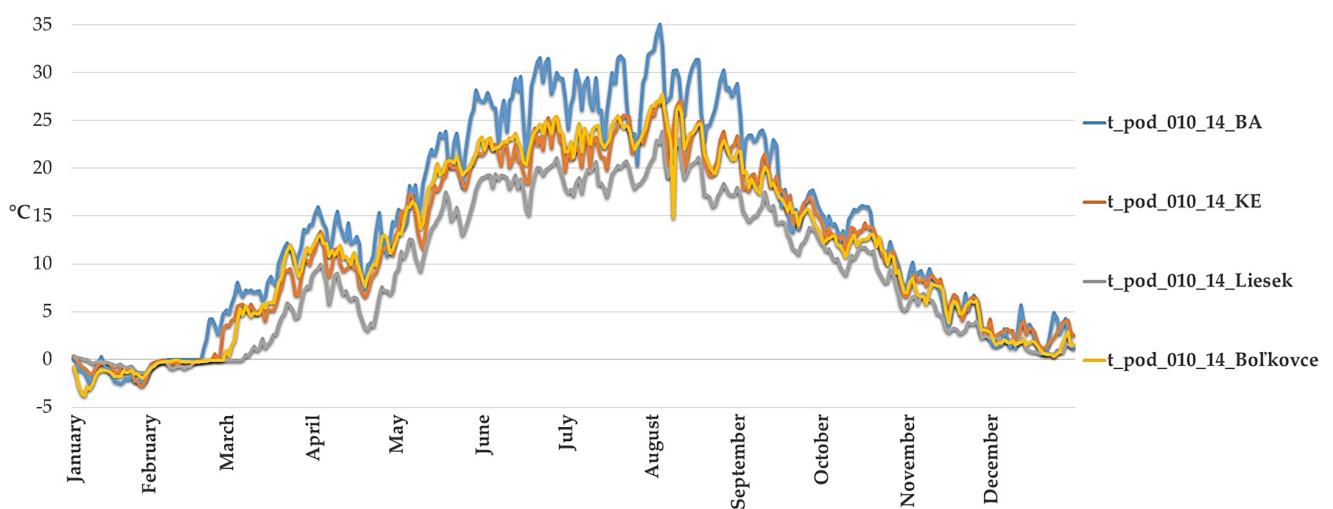


**Figure 3.** Soil temperature fluctuations at a depth of 10 cm during the year in Bratislava (BA), Košice (KE), Liesek, and Boľkovce (°C) [21,22].

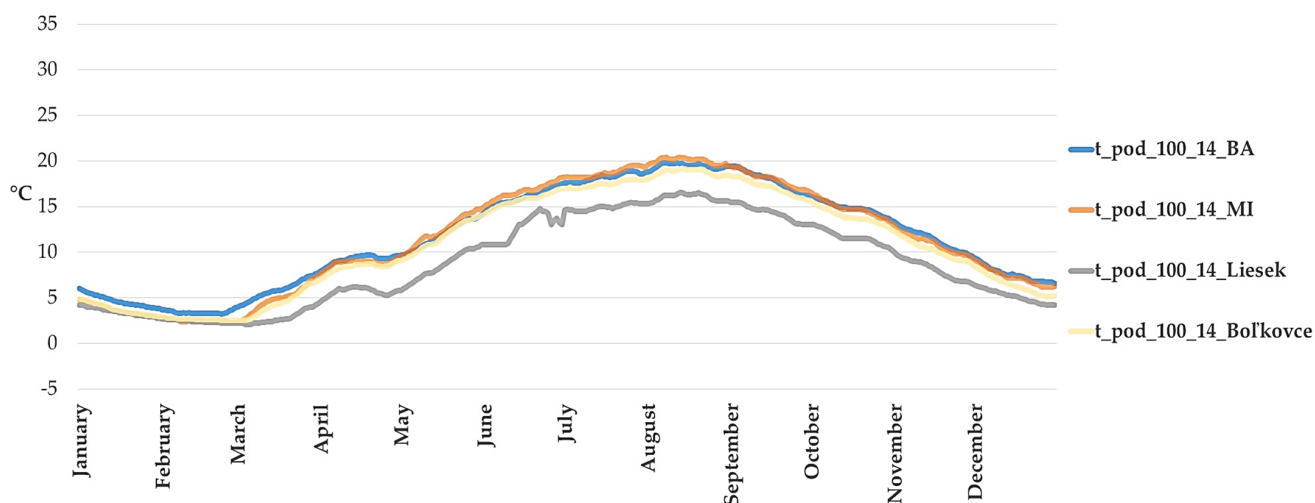


Figure 4. Soil temperature fluctuations at a depth of 100 cm during the year in Bratislava, Michalovce, Liesek, and Bol'kovce (°C) [21,22].

Table 6. Average soil temperatures at 10 cm and 100 cm depth during 2017 [21,22].

Place of Measure	10 cm				100 cm			
	March – May	June – August	September – November	December – February	March – May	June – August	September – November	December – February
Bratislava	14 °C	27.9 °C	13.1 °C	0.6 °C	9 °C	19.9 °C	15 °C	4.9 °C
Košice	11.2 °C	22.6 °C	12.2 °C	0.6 °C	Data not available			
Michalovce	12.7 °C	23.8 °C	12.6 °C	0.3 °C	8.6 °C	15.3 °C	14.6 °C	4.6 °C
Bol'kovce	11.9 °C	23.3 °C	11.6 °C	−0.1 °C	8.1 °C	17.3 °C	13.8 °C	4.3 °C
Liesek	7.7 °C	19.1 °C	9.5 °C	0.2 °C	5.7 °C	15.5 °C	11.4 °C	3.7 °C
Average	11.5 °C	23.3 °C	11.8 °C	0.3 °C	7.9 °C	17.0 °C	13.7 °C	4.4 °C

Knowing the type of soil and grain size of the soil is very important for the installation of horizontal ground collectors, as it can significantly affect its operation and performance. Figure 5 expresses what percentage of the territory of the Slovak Republic has which type of soil, and in Figure 6, the percentage of types of soil according to grain size is shown.

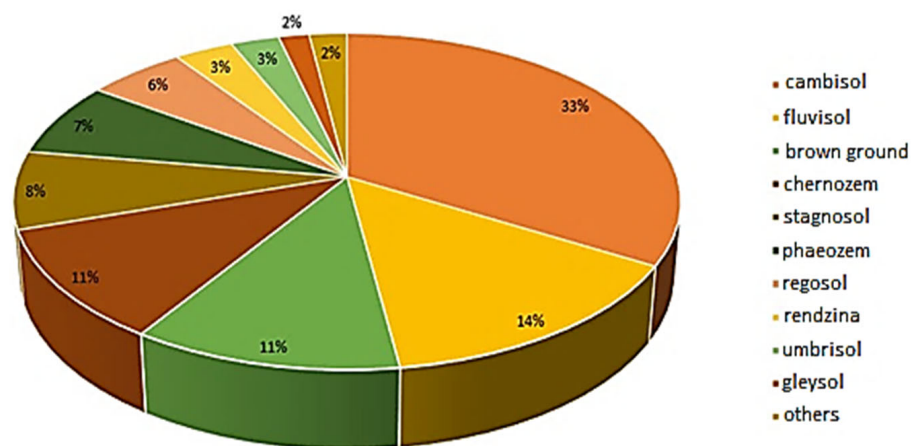
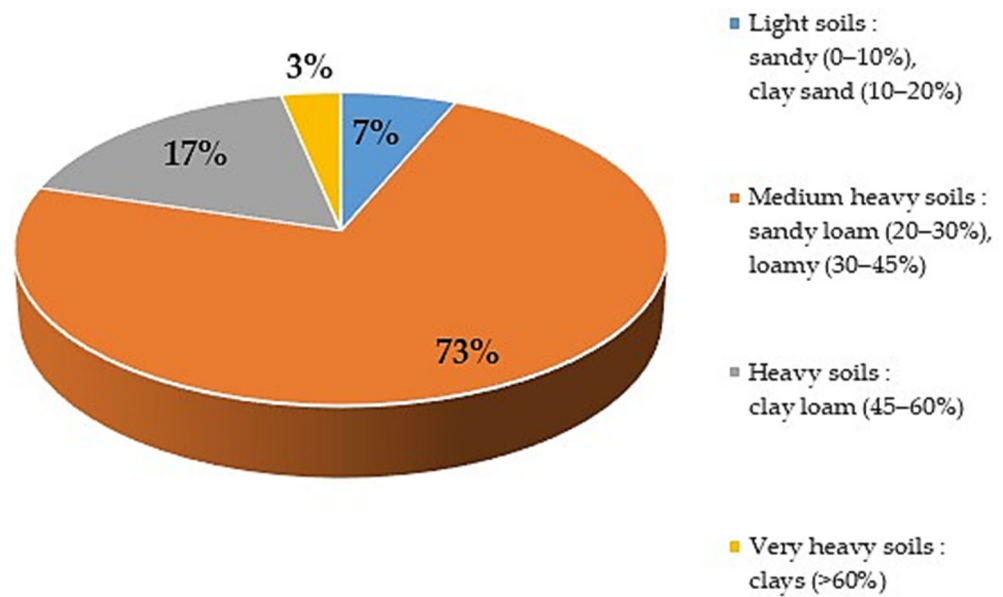


Figure 5. Type of soil in Slovakia [20].



**Figure 6.** Soil types by grain size in Slovakia [20].

Although there is an assumption that our results could be affected by the latent heat of the phase change by thermal gradient and migration of moisture, this was not a consideration in this paper. Firstly, in case 1 with the meander collector, we aimed to find out the impact of different soil types on the performance of the collector; the types of soil and their properties are described in Table 7. A mixture of ethylene glycol and water in the ratio of 30: 70 was used in simulations. In Table 8, the working medium properties are shown. The pipe material used in this research was HDPE, the properties set up in simulations are shown in Table 9.

**Table 7.** Average temperatures of soils in Slovakia and their properties used in simulations [19–22].

Period	10 cm Depth	100 cm Depth
March–May	11.5 °C	7.9 °C
September–November	11.8 °C	13.7 °C
December–February	0.3 °C	4.4 °C

Type of Soil	Specific Heat Capacity (J·kg <sup>-1</sup> ·K <sup>-1</sup> )	Density (kg·m <sup>-3</sup> )	Coefficient of Thermal Conductivity (W·m <sup>-1</sup> ·K <sup>-1</sup> )
Dry soil—sand	800	1600	0.7
Moist soil—sand	1100	2000	1.4
Saturated soil—sand	1350	2000	2.8
Dry soil—clay	1000	1600	1
Wet soil—clay	1300	2000	1.5

**Table 8.** Properties of the working medium used in simulations [23].

Collectors' medium	Water + Ethylene glycol (70:30)
Inlet temperature	−4 °C
Density	1049 kg·m <sup>-3</sup>
Specific heat capacity	3669 J·kg <sup>-1</sup> ·K <sup>-1</sup>
Coefficient of thermal conductivity	0.432 W·m <sup>-1</sup> ·K <sup>-1</sup>
Dynamic viscosity	5.096·10 <sup>-3</sup> Pa·s <sup>-1</sup>
Flow velocity	0.1 m·s <sup>-1</sup>

**Table 9.** Properties of HDPE pipe used in simulations.

Outer/inner diameter	0.044/0.040 m
Specific heat capacity	2450 J·kg <sup>-1</sup> ·K <sup>-1</sup>
Density	950 kg·m <sup>-3</sup>
Coefficient of thermal conductivity	0.42 W·m <sup>-1</sup> ·K <sup>-1</sup>

The values of parameters such as pipe diameter, flow velocity in the pipe, and the choice of a 7:3 mixture of water and ethylene glycol as the working medium, among others, were determined in the simulation in consultation with practitioners. The selected values are used in the Slovak Republic for heat pump installations.

After simulations with the meander collector were done, authors ran simulations with their own designs, the vertical spiral, with three different diameters (6, 8, and 10 m), depth of installation, length of pipe, and spacing in a vertical direction.

The continuity equation or equation for conservation of mass used in this research can be written as follows:

$$\frac{\partial \rho}{\partial t} + \nabla \cdot (\rho \vec{v}) = S_m \quad (1)$$

The equation for the conservation of momentum in an inertial (non-accelerating) reference frame is

$$\frac{\partial}{\partial t} (\rho \vec{v}) + \nabla \cdot (\rho \vec{v} \vec{v}) = -\nabla p + \nabla \cdot (\overline{\overline{T}}) + \rho \vec{g} + \vec{F} \quad (2)$$

where  $p$  is the static pressure and  $\rho \vec{g}$  and  $\vec{F}$  are the gravitational body force and external body forces.

The equation for stress tensor  $\overline{\overline{T}}$  can be written as follows:

$$\overline{\overline{T}} = \mu \left[ \left( \nabla \vec{v} + \nabla \vec{v}^T \right) - \frac{2}{3} \nabla \cdot \vec{v} I \right] \quad (3)$$

where  $\mu$  is the molecular viscosity,  $I$  is the unit tensor, and the second term on the right-hand side is the effect of volume dilation.

The equation for the conservation of energy is

$$\frac{\partial}{\partial t} (\rho E) + \nabla \cdot (\vec{v} (\rho E + p)) = -\nabla \cdot \left( \sum_j h_j J_j \right) + S_h \quad (4)$$

Then, the value of outlet temperatures was found and the following equation was used for calculation of the collector's output:

$$P = \rho \times C_p \times u \times A \times (T_{out} - T_{in}) \quad (5)$$

where  $\rho$  represents the density of the medium,  $C_p$  is the specific heat capacity at constant pressure,  $u$  is inlet velocity,  $A$  is the cross-sectional area of the pipe, and  $(T_{out} - T_{in})$  represents the temperature difference at the inlet and outlet of the collector [24].

In the end, specific power (W per 1 m of pipe and W per 1 m<sup>2</sup> of land) was determined by divided results of (5), firstly with the length of pipe and then with the area of the collector. All results from numerical simulations were processed into graphs and maps of temperature distribution around the collectors, which serve to compare all the geometries and show if the authors' designs' outputs achieved the output of the classical geometry—meander [25].

### 3. Results of Research

This section corresponds to the workflow in Table 1 and shows the results in order of cases 1 to 5.

### 3.1. Case 1—Meander

The effect of different contents of water in the same type of soil is shown in Figure 7. It is evident that more saturated soil has a better heat capacity and conductivity, while in drier soil, heat extraction is not so smooth and there is a problem with greater cooling between rows of pipe.

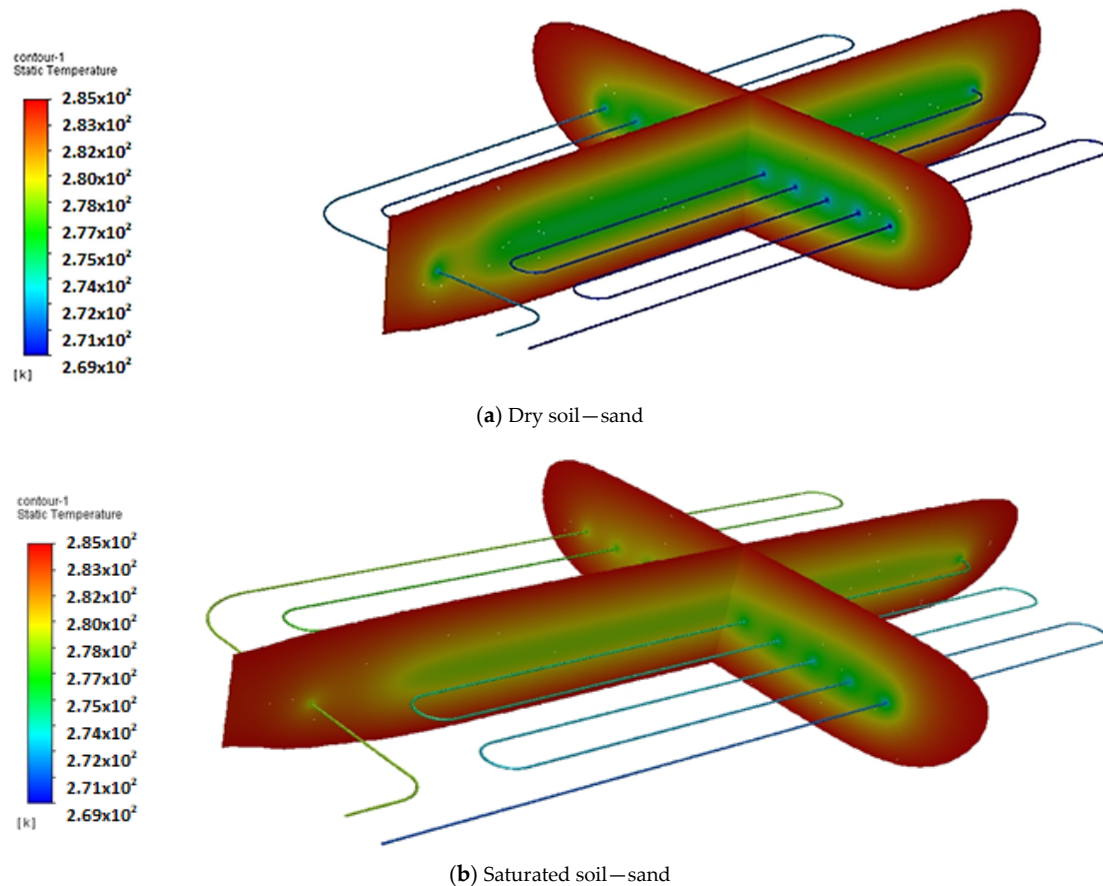


**Figure 7.** Distribution of temperatures in soils with different contents of water with the meander geometry collector.

### 3.2. Case 2—Spiral $\varnothing$ 6 m, 3.75 Coils

In general, the difference between the meander output and this geometry output is noticeable. While the new design has a worse performance than the meander, this could be caused by a difference in length (the length of case 1 is 142 m, the length of case 2 is just 102 m (−28.16%)). Another problem could be the spacing between the pipes in vertical and horizontal directions, which causes negative mutual thermal influence.

### 3.3. Case 3—Spiral $\varnothing$ 6 m, 2.75 Coils

To improve the previous geometry, one loop of pipe was removed, which made spacing in the vertical direction greater, from 0.8 to 1.27 m, but the pipe was shortened to 67.4 m (−52.53%). If we would like to achieve a higher performance of this geometry, we should make this spiral deeper and use a longer tube, because now this design is not as effective as the meander geometry.

### 3.4. Case 4—Spiral $\varnothing$ 8 m, 3.75 Coils

Due to a still-low performance, the diameter of the coil (from 6 to 8 m) and the length of the pipe (from 67.4 to 115.24 m) increased. On the other hand, the depth of installation was reduced from 3.5 m to 2 m. The vertical direction was 0.53 m. The results of this

geometry are closer to the results of the meander than in previous cases, but the vertical influence between pipes was considerable.

### 3.5. Case 5—Spiral $\varnothing$ 10 m, 3.75 Coils

In this case, a vertical spiral collector with a 10 m diameter operation was simulated. This collector was 133.8 m long, which is 8.7 m (5.77%) shorter than the meander in case 1. The spacing between layers of the pipe was 0.53 m again, which could be the reason for the significant vertical influence and mutual cooling of the pipes, but the bigger diameter eliminated the horizontal influence of the pipes (Figure 8). Table 10 shows the specific simulation results in the form of the outlet temperatures obtained in Fluent. The daily trends of temperature were the same for all types of soil.

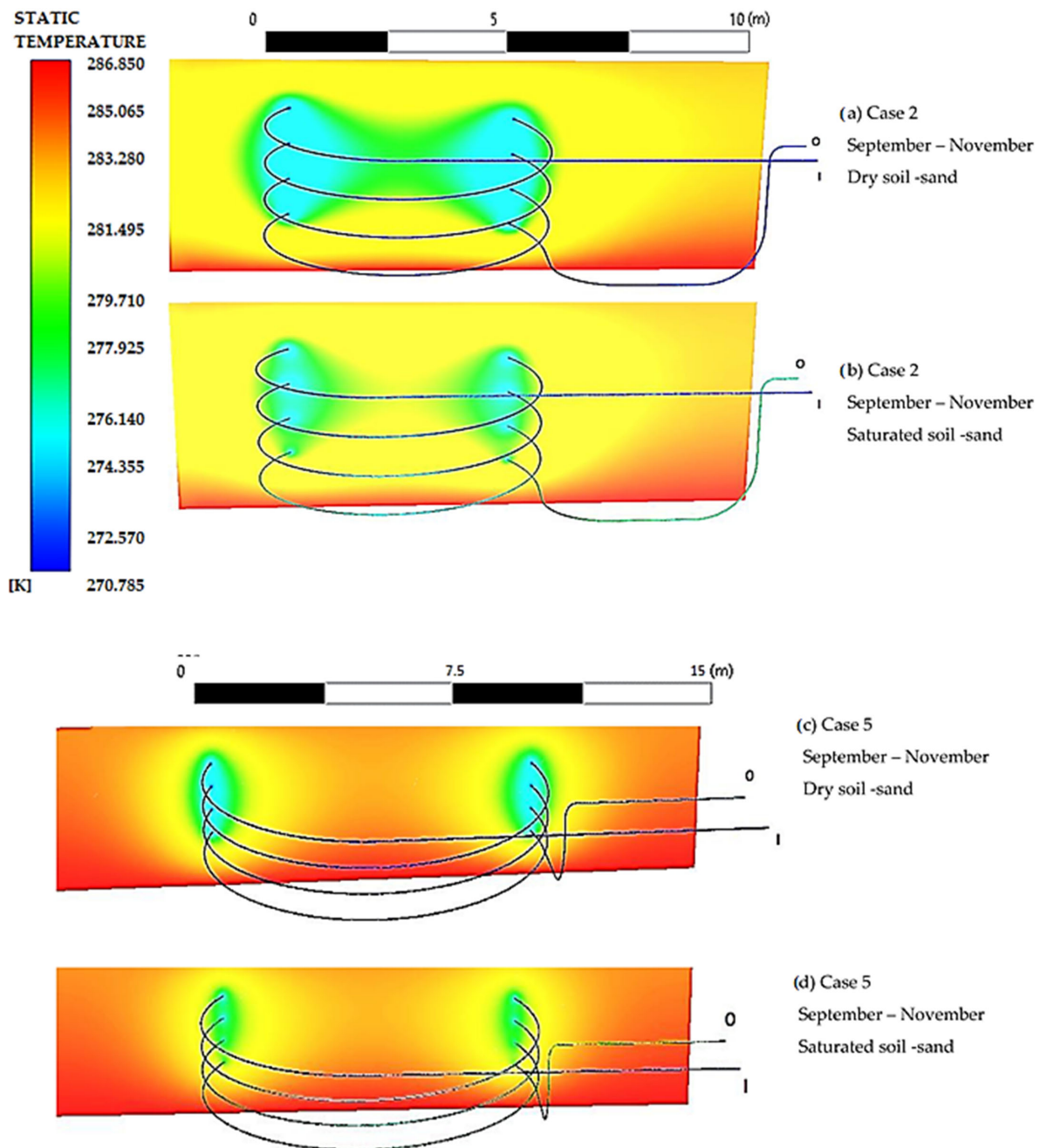


**Figure 8.** Distribution of temperatures in soils with different contents of water with vertical spiral geometry collector.

**Table 10.** Outlet temperature—results of simulations.

Daily Trends of Temperature (K)	Outlet Temperature (K)				
	Meander	Spiral 6 m 3.75	Spiral 6 m 2.75	Spiral 8 m	Spiral 10 m
Dry sand, gravel					
September–October–November (290.4–286.9–282.9)	272.39	271.01	271.01	271.41	272.02
December–January–February (279.2–275.9–275.0)	270.40	269.85	269.87	270.00	270.19
March–April–May (277.9–281.6–285.4)	271.8	270.71	270.63	271.09	271.49
Moist sand					
September–November	274.88	272.59	272.58	273.24	274.28
December–February	271.36	270.46	270.45	270.65	271.05
March–May	273.86	272.00	271.92	272.58	273.44
Saturated sand, gravel					
September–November	278.36	275.10	275.05	276.17	277.54
December–February	272.69	271.43	271.45	271.73	272.25
March–May	276.70	274.05	273.89	274.92	276.11
Dry clay					
September–November	273.54	271.72	271.72	272.29	273.05
December–February	270.84	270.12	270.14	270.29	270.58
March–May	272.75	271.28	271.23	271.74	272.42
Wet clay					
September–November	275.19	272.80	272.79	273.62	274.57
December–February	271.47	270.54	270.55	270.76	271.14
March–May	274.10	272.16	272.09	272.78	273.67

Figure 9 shows the  $\Delta T$  values obtained by subtracting the inlet temperature, which was 269.15 K in all cases, from the outlet temperature (the values in Table 10).

In agreement with other studies of this kind, we found a significant influence of the soil environment on the collector both in terms of soil type and soil water content, as it can be seen in Figures 9–11. The collector performance was 37.5–184.9% higher in wet soils than in dry soils. The difference in collector performance in different soil types was about 5% between wet clay and wet sand in favor of clay, almost 36% between dry sand and dry clay, better for clay, and in saturated sand, gravel had a performance of 52.5% higher than in wet clay.

The results of the second case (vertical spiral with 6 m diameter, depth 4 m) were not gratifying, because the performance of this case was poorer than the performance of the meander in total by 19.8–44%, and per 1 m output of vertical spiral, it was lower by 17.7–29%. However, we must take into account that the pipe length for this collector was shorter by 28.4%. There is significant two-sided temperature impact, in the horizontal as well as the vertical direction, which makes this system inefficient.

In the third case (vertical spiral with 6 m diameter, depth 4.5 m), to make the system more effective, the space between pipes was boosted from 0.8 m to 1.27 m. The results show that the desired effect was achieved and the influence of one part of the pipeline on another was reduced. However, running this installation was still less efficient than the meander by 35–44% in total and by 19–29% per 1 m of pipe.

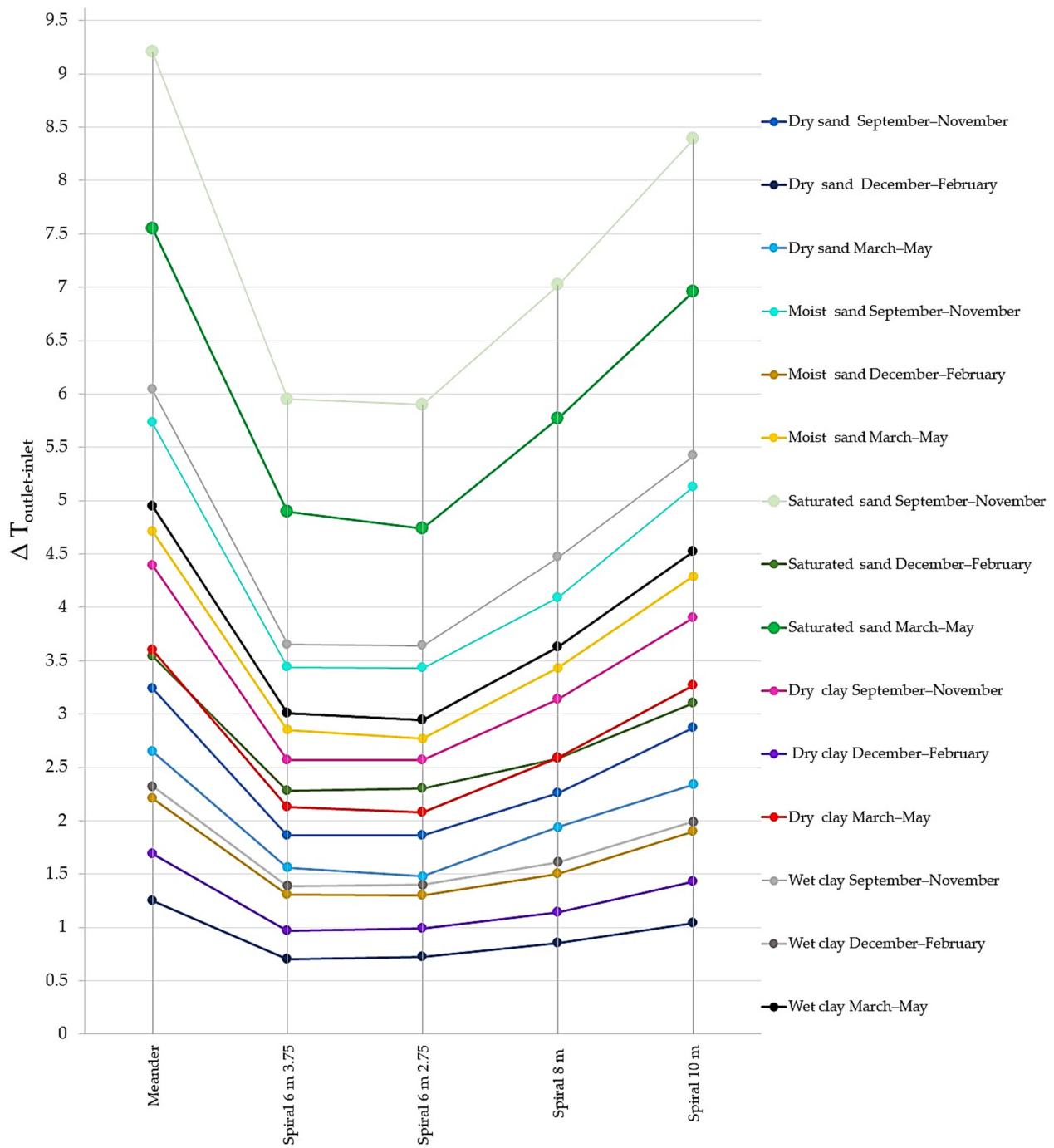


Figure 9. Results of dividing the outlet and inlet temperature of the simulations  $\Delta T_{\text{outlet-inlet}}$ .

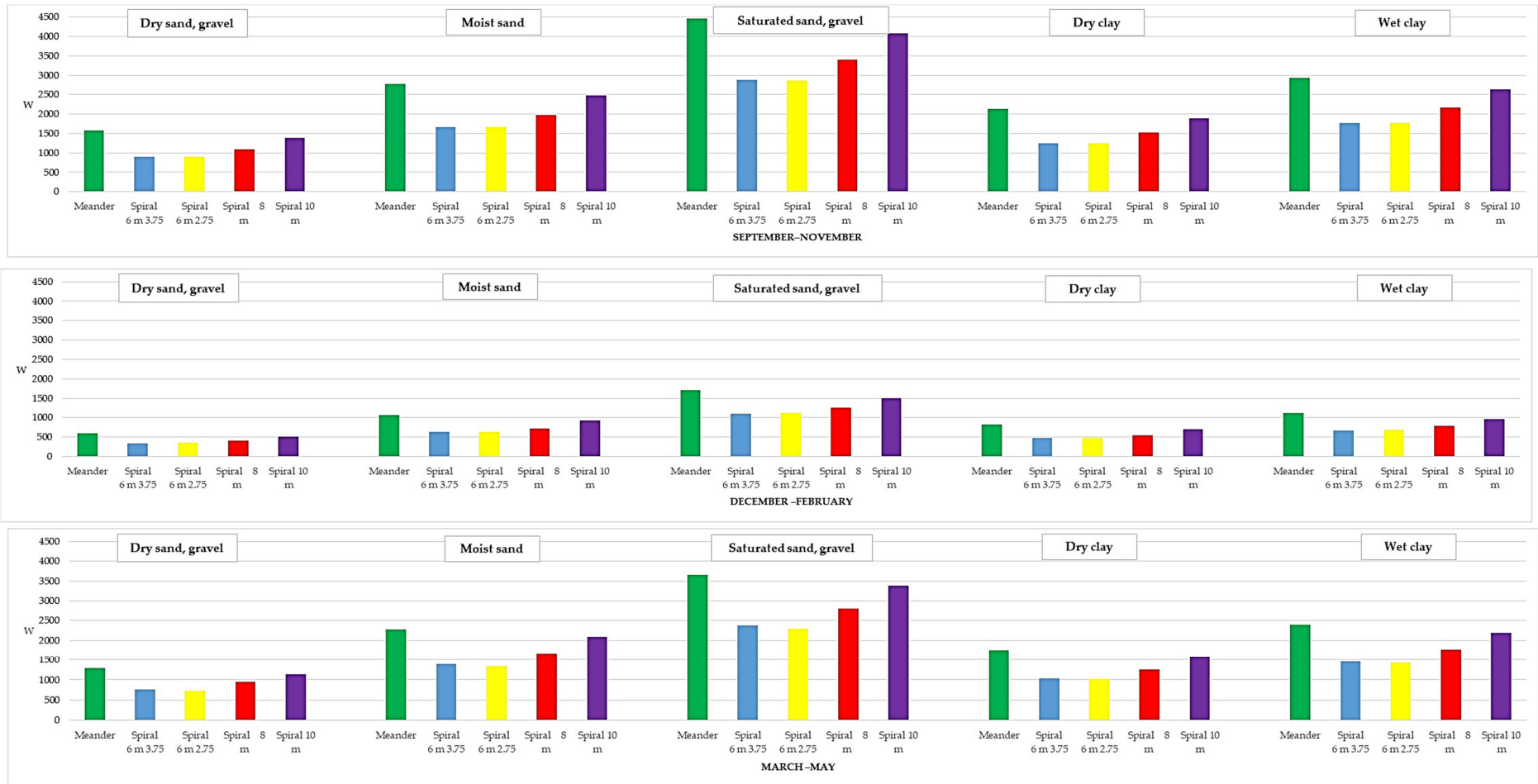


Figure 10. Total output of collectors  $P_T$ , cases 1–5.

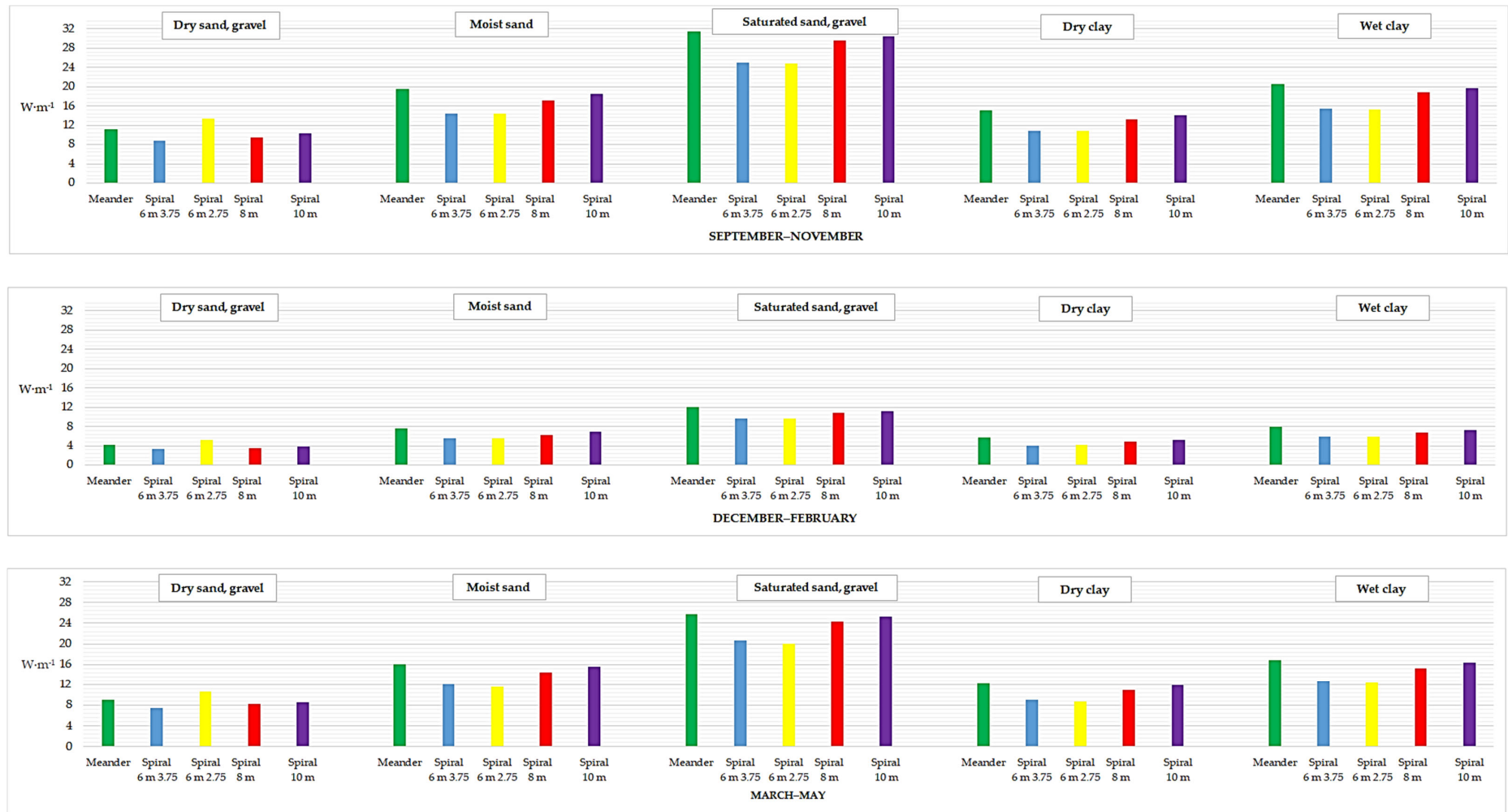


Figure 11. The specific performance for 1 m of collector pipe, cases 1–5.

In the fourth case (vertical spiral with 8 m diameter), the diameter of the coil was bigger by 2 m than in cases 2 and 3, but the space between pipes was decreased from 1.27 m to 0.53 m. This could be reason why the temperature harvesting of this setup was smaller than in the meander case by 23–32.5% (5–16.6% per 1 m), see Figures 9–11.

At the end, the installation with the biggest diameter (10 m) was simulated and in spite of lower effectivity against the meander (−7% up to −16.8% in total, −1.8% up to −11.4% per 1 m), this work can be considered as filling a big gap in the field of vertical spiral collectors. The reciprocal effect between pipes in the horizontal direction was reduced, but in the vertical direction, it was still considerable. Limitations by size installation area can occur.

The results of all simulations are shown in Figures 10 and 11. From these results, it is obvious that collectors in soils with a content of water have a higher output (37.5–184.9%) than those in dry soils. On the other hand, the type of soil and its thermophysical behavior also has a significant effect on the output of the collector; the difference can be from 5% between wet clay and moist sand, to 52.5% between wet clay and saturated sand. The next figures show comparisons between the total output of every geometry and installation during each period in all types of soil. It is clear from Figure 10 that none of our designs match the performance of the classical meander geometry, but the design from case 5 is very close to this. To better compare the collector performance due to its varied length, comparisons in Figure 11 are per 1 m of pipe.

#### 4. Discussion

The technological development of heat pump collectors and their optimization are an essential part of the faster implementation of heat pumps in the energy mix of today. This includes finding a solution for ground collectors, which require a large area for their installation, which is difficult to find, especially in cities, as well as people in rural areas possibly not being willing to have their land encroached on to such a large extent. Therefore, the authors of the paper came up with the design of a vertical spiral, the efficiency of which was investigated and compared using numerical simulation with the classical meander geometry. The installation of the new geometry could proceed as follows (Figure 12):

1. A pit would be dug in a circular pattern, with a reasonable depth of 2–4.5 m, possibly a little more.
2. The collector would be laid while continuously backfilling the already laid pipe.

After consultation with the company ENVIGEO a.s., the proposal for the implementation of the installation of the new geometry is to drill holes to a depth of about 6 m with a drilling diameter of 630 mm with a drilling rig PVSD—Zubor. Drilling will take place under suitable geological conditions with a grab with a 630 mm diameter attachment without continuous casing. In the event that geological conditions require casing, this rig is equipped with a 30 m string of casings with quick couplings based on studs. In this case, after the installation of polyethylene hoses and filling them with sand, the casings were pulled out of the well, and sand was added instead of the volume of the casings.

According to the price list of ENVIGEO a.s. the price for digging a borehole with a diameter of 630 mm up to 15 m is 180–249 EUR per meter plus sand and hoses. Therefore, the cost of installing a vertical spiral collector would be

- Ø 6 m. . . . . 3384–4681.2 EUR + sand + hoses
- Ø 8 m. . . . . 4518–6249.9 EUR + sand + hoses
- Ø 10 m. . . . . 5652–7818.6 EUR + sand + hoses

This method does not require digging up and moving large amounts of soil (Figure 12), nor does it need a 30–300 m borehole like with earth probes, which can save costs and time. It also does not restrict the landowner to the same extent as during and after installing a collector with a meander geometry.

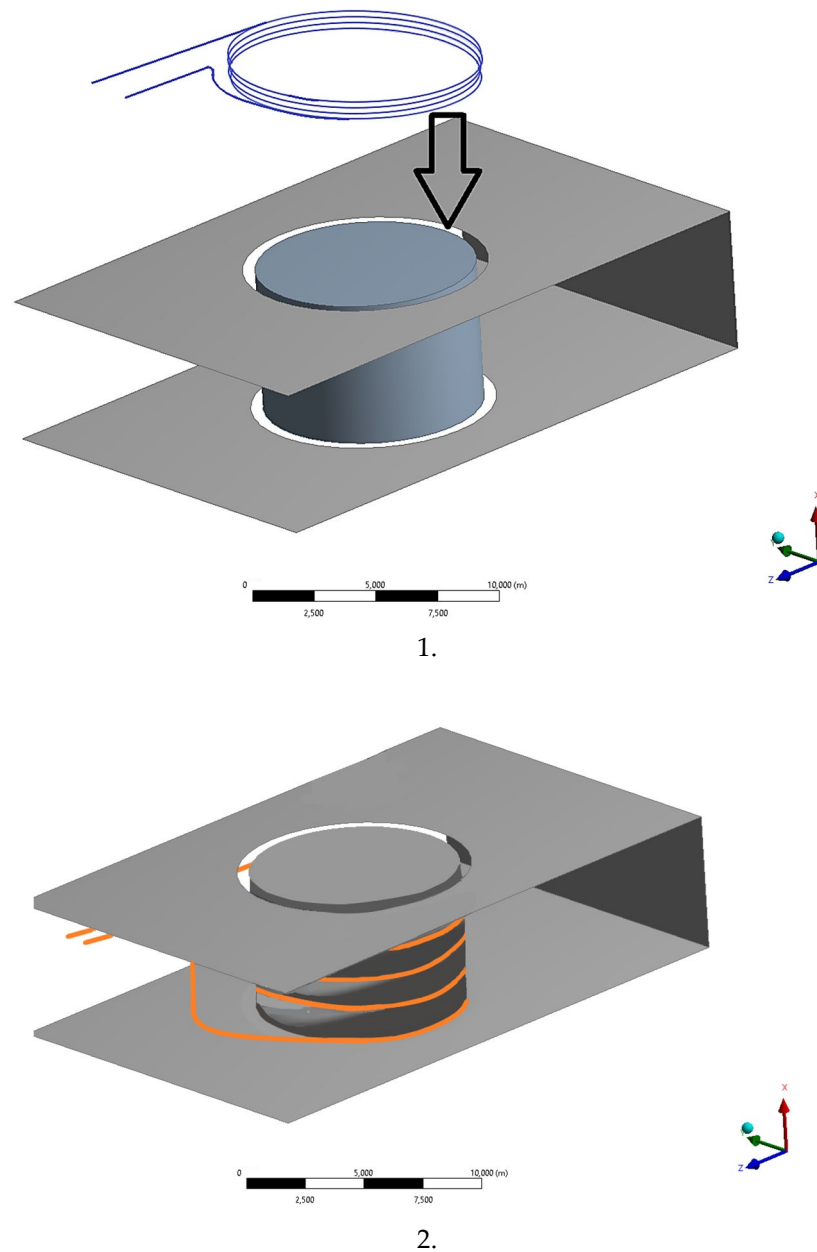


**Figure 12.** Installation of vertical spiral collector, 1. stowage of collector, 2. final state.

The results in Section 3 show that none of the designs of the authors of the current paper showed an overall performance higher than that of the meander design, although the designs in cases 4 and 5 achieved more than 75% of the output of the meander collector (23.7–32% difference). Only in one case was the performance of the spiral collector per 1 m of pipe higher than that of the meander, namely for the 6 m, 2.75 coils spiral (+17.56%); otherwise, even in that case, only spirals of 8 (difference 5.74–15.76%) and 10 m (difference 2.97–11.29%) were close in performance.

We also found that soil type and its water content can cause large differences in the performances of the same geometry, which is in accordance with other works of this kind. Moreover, it was confirmed that in the territory of Slovakia, the soil has the greatest heating potential in the period September–November, when the accumulated heat from the summer months is stored even at a depth of 100 cm or more.

## 5. Conclusions

In this article, we examined heat exchangers, also called ground collectors, and confirmed the factors (type of soil, geometry) that have the biggest influence on their operation and output, as a lot of other studies stated. We investigated how the geometrical and spatial distribution affect the total output of these systems and also their collectors' surrounding ground environment energy balance.

In agreement with other studies of this kind, we found a significant influence of the soil environment on the collector, both in terms of soil type and soil water content.

The work also included a new geometry, the authors' own proposal, that would reduce the collector area, possibly reducing the amount of excavation and earthwork required to place the collector in the soil, and increase the collector efficiency. Despite the output of these designs not reaching the values of conventional geometry, the results are worthy of consideration and such placement can be considered in specific cases. The research on ground collectors and their geometry should not be undervalued, especially if there is serious interest in the acceleration of the implementation of heat pumps for heating in cities and metropolises and increasing their usage.

This research shows that the best geometry of our designs is the spiral of 10 m diameter, which almost matches the performance of the meander geometry.

**Author Contributions:** Resources, L.G.; conceptualization, L.G.; methodology, L.G.; software, L.G.; data curation, L.G.; writing—original draft preparation, L.G.; visualization, L.G.; writing—review and editing, L.G.; validation, D.K.; investigation, D.K.; project administration, D.K.; funding acquisition, D.K.; formal analysis, D.K.; supervision, D.K. All authors have read and agreed to the published version of the manuscript.

**Funding:** This research was funded by the European Regional Development Fund, Research on the impact of the implementation of alternative energy sources in the energy management processes of industries/ITMS: 313011T564.

**Data Availability Statement:** Not applicable.

**Conflicts of Interest:** The authors declare no conflict of interest. The funders had no role in the design of the study, in the collection, analyses, or interpretation of data; in the writing of the manuscript, or in the decision to publish the results.

## References

1. IEA. HPT: ETP 2017 Shows that Heat Pumps Will Be One of the Key Technologies for the Building Sectors in the 2BDS. 2017. Available online: <https://heatpumpingtechnologies.org/etp2017-heat-pumps-key-technologies-building-sectors/> (accessed on 14 September 2020).
2. IEA. Share of Households Purchasing Heat Pumps for Heating and Hot Water Production in Selected Regions the Sustainable Development Scenario, 2010–2030. 2020. Available online: <https://www.iea.org/reports/heat-pumps> (accessed on 14 September 2020).
3. Bhutta, M.M.A. CFD Applications in Various Heat Exchangers Design: A Review. *Appl. Therm. Eng.* **2012**, *32*, 1–12. Available online: <https://www.sciencedirect.com/science/article/pii/S1359431111004807> (accessed on 20 February 2020).
4. Hepburn, B.D.P.; Sedighi, M.; Thomas, H.R.; Manju. Field-scale monitoring of a horizontal ground source heat system. *Geothermics* **2016**, *61*, 86–103. Available online: <https://www.sciencedirect.com/science/article/pii/S0375650516000146> (accessed on 24 February 2019). [CrossRef]
5. Benazza, A.; Blanco, E.; Aichouba, M.; Río, J.L.; Laouedj, S. Numerical Investigation of Horizontal Ground Coupled Heat Exchanger. *Energy Procedia* **2011**, *6*, 29–35. Available online: <https://cyberleninka.org/article/n/1221350.pdf> (accessed on 24 February 2019). [CrossRef]
6. del-Castillo-García, G.; Borinaga-Treviño, R.; Sañudo-Fontaneda, L.A.; Pascual-Muñoz, P. Influence of pervious pavement systems on heat dissipation from a horizontal geothermal system. *Eur. J. Environ. Civ. Eng.* **2013**, *17*, 956–967. Available online: [https://www.researchgate.net/publication/257222793\\_Influence\\_of\\_Pervious\\_Pavement\\_Systems\\_on\\_heat\\_dissipation\\_from\\_a\\_horizontal\\_geothermal\\_system](https://www.researchgate.net/publication/257222793_Influence_of_Pervious_Pavement_Systems_on_heat_dissipation_from_a_horizontal_geothermal_system) (accessed on 24 February 2019). [CrossRef]
7. Sanaye, S.; Niroomand, B. Simulation of heat exchanger network (HEN) and planning the optimum cleaning schedule. *Energy Convers. Manag.* **2007**, *48*, 1450–1461. Available online: <https://www.sciencedirect.com/science/article/pii/S0196890406003724> (accessed on 24 February 2019). [CrossRef]

8. Chong, C.S.A.; Gan, G.; Verhoef, A.; Garcia, R.G.; Vidale, P.L. Simulation of thermal performance of horizontal slinky-loop heat exchangers for ground source heat pumps. *Appl. Energy* **2013**, *104*, 603–610. Available online: <https://www.sciencedirect.com/science/article/pii/S0306261912008744> (accessed on 23 February 2019). [CrossRef]
9. Congedo, P.M.; Colangelo, G.; Starace, G. CFD simulations of horizontal ground heat exchangers: A comparison among different configurations. *Appl. Therm. Eng.* **2012**, *33–34*, 24–32. Available online: <https://www.sciencedirect.com/science/article/pii/S135943111004856> (accessed on 24 February 2019). [CrossRef]
10. Congedo, P.M.; Colangelo, G.; Starace, G. Horizontal Heat Exchangers for GSHP. Efficiency and Cost Investigation for Three Different Applications. In *STARACE. CONGEDO a COLANGELO, Proceedings of the ECOS2005–18th International Conference on Efficiency. Cost. Optimization. Simulation and Environment, Trondheim, Norway, 20–22 June 2005*; Tapir Academic Press: Trondheim, Norway, 2005; Available online: [https://www.researchgate.net/profile/Gianpiero\\_Colangelo/publication/257277153\\_Horizontal\\_Heat\\_Exchangers\\_for\\_GSHP\\_Efficiency\\_and\\_Cost\\_Investigation\\_for\\_Three\\_Different\\_Applications/links/54db5e0d0cf261ce15cffe7b.pdf](https://www.researchgate.net/profile/Gianpiero_Colangelo/publication/257277153_Horizontal_Heat_Exchangers_for_GSHP_Efficiency_and_Cost_Investigation_for_Three_Different_Applications/links/54db5e0d0cf261ce15cffe7b.pdf) (accessed on 5 April 2019).
11. Capozza, A.; Zarrella, A.; De Carli, M. Long-term analysis of two GSHP systems using validated numerical models and proposals to optimize the operating parameters. *Energy Build.* **2015**, *93*, 50–64. Available online: <https://www.sciencedirect.com/science/article/pii/S0378778815000997> (accessed on 24 February 2019). [CrossRef]
12. Wu, Y.; Gan, G.; Verhoef, A.; Vidale, P.L.; Gonzalez, R.G. Experimental measurement and numerical simulation of horizontal-coupled slinky ground source heat exchangers. *Appl. Therm. Eng.* **2010**, *30*, 2574–2583. Available online: <https://www.sciencedirect.com/science/article/pii/S1359431110002917> (accessed on 24 February 2019). [CrossRef]
13. Go, G.-H.; Lee, S.-R.; Yoon, S.; Kim, M.-J. Optimum design of horizontal ground-coupled heat pump systems using spiral-coil-loop heat exchangers. *Appl. Energy* **2016**, *162*, 330–345. Available online: <https://www.sciencedirect.com/science/article/pii/S0306261915013495> (accessed on 24 February 2019). [CrossRef]
14. Yoon, S.; Lee, S.R.; Go, G.-H. Evaluation of thermal efficiency in different types of horizontal ground heat exchangers. *Energy Build.* **2015**, *105*, 100–105. Available online: <https://www.sciencedirect.com/science/article/pii/S0378778815301717> (accessed on 24 February 2019). [CrossRef]
15. Kim, M.-J.; Lee, S.-R.; Yoon, S.; Go, G.-H. Thermal performance evaluation and parametric study of a horizontal ground heat exchanger. *Geothermics* **2016**, *60*, 134–143. Available online: <https://www.sciencedirect.com/science/article/pii/S0375650515001649> (accessed on 24 February 2019). [CrossRef]
16. Kudelas, D.; Taušová, M.; Tauš, P.; Gabániová, L.; Koščo, J. Investigation of Operating Parameters and Degradation of Photovoltaic Panels in a Photovoltaic Power Plant. *Energies* **2019**, *12*, 3631. [CrossRef]
17. Cirillo, L.; Greco, A.; Masselli, C. Computational investigation on daily, monthly and seasonal energy performances and economic impact through a detailed 2D FEM model of an earth to air heat exchanger coupled with an air conditioning system in a continental climate zone. *Energy Build.* **2023**, *296*, 113365. [CrossRef]
18. Liu, Q.; Tao, Y.; Shi, L.; Zhou, T.; Huang, Y.; Peng, Y.; Wang, Y.; Tu, J. Parametric optimization of a spiral ground heat exchanger by response surface methodology and multi-objective genetic algorithm. *Appl. Therm. Eng.* **2023**, *221*, 119824. [CrossRef]
19. Adamovský, R.; Neuberger, P.; Kodešová, R. *Metodika pro Využití Půdy Jako Nízkoteplotního Zdroje Energie Tepelných Čerpadel: Certifikovaná Metodika*; ČZU: Praha, Czech Republic, 2015; 29p.
20. SOIL PORTAL. Available online: [http://www.podnemapy.sk/portal/verejnost/obj\\_hmotnost/obj\\_hmotnost.aspx](http://www.podnemapy.sk/portal/verejnost/obj_hmotnost/obj_hmotnost.aspx) (accessed on 24 October 2020).
21. Slovak Hydrometeorological Institute. *Soil Temperatures 2008–2017; Measurement Stations of the Slovak Republic*: Bratislava, Slovakia, 2019.
22. SHMU. *Bulletin Meteorology and Climatology of Slovakia*; Slovak Hydrometeorological Institute: Bratislava, Slovakia, 2018; Volume 24, ISSN 1337-5458. Available online: [http://www.shmu.sk/File/ExtraFiles/KMIS/publikacie/BMaK\\_0518.pdf](http://www.shmu.sk/File/ExtraFiles/KMIS/publikacie/BMaK_0518.pdf) (accessed on 27 February 2019).
23. Füre, B.; (Slovak University of Technology, Bratislava, Slovakia). Personal Communication. 2018.
24. Han, C.; Yu, X. Sensitivity analysis of a vertical geothermal heat pump system. *Appl. Energy* **2016**, *170*, 18. Available online: <https://www.sciencedirect.com/science/article/abs/pii/S0306261916302252> (accessed on 9 April 2020). [CrossRef]
25. Wittenberger, G.; Sofranko, M. Formation and protection against incrustation on the geothermal pipe by utilizing of geothermal water in the area of Durkov (Eastern Slovakia). *Acta Montan. Slovaca* **2015**, *20*, 10–15. Available online: <https://actamont.tuke.sk/pdf/2015/n1/2wittenberger.pdf> (accessed on 17 July 2021).

**Disclaimer/Publisher’s Note:** The statements, opinions and data contained in all publications are solely those of the individual author(s) and contributor(s) and not of MDPI and/or the editor(s). MDPI and/or the editor(s) disclaim responsibility for any injury to people or property resulting from any ideas, methods, instructions or products referred to in the content.